P. M. Jordan; J. K. Fulford
A note on poroacoustic traveling waves under Darcy's law: Exact solutions

Applications of Mathematics, Vol. 56 (2011), No. 1, 99–115

Persistent URL: http://dml.cz/dmlcz/141408

56 (2011) APPLICATIONS OF MATHEMATICS No. 1, 99–115

A NOTE ON POROACOUSTIC TRAVELING WAVES UNDER DARCY'S LAW: EXACT SOLUTIONS*

P. M. Jordan, J. K. Fulford, Stennis Space Center

Dedicated to Professor K. R. Rajagopal on the occasion of his 60th birthday

Abstract. A mathematical analysis of poroacoustic traveling wave phenomena is presented. Assuming that the fluid phase satisfies the perfect gas law and that the drag offered by the porous matrix is described by Darcy's law, exact traveling wave solutions (TWS)s, as well as asymptotic/approximate expressions, are derived and examined. In particular, stability issues are addressed, shock and acceleration waves are shown to arise, and special/limiting cases are noted. Lastly, connections to other fields are pointed out and possible extensions of this work are briefly discussed.

Keywords: poroacoustics, Darcy's law, traveling waves, shock and acceleration waves

MSC 2010: 33E30, 35L67, 76N15, 76S05

1. Introduction

The study of acoustic propagation in fluid-saturated porous media, often referred to as poroacoustics, is an important sub-field of acoustics that dates back many years; see, e.g., [13], [22], [14], [23] and references therein. Some recent contributions to this field include Rajagopal and Tao's [20] elegant, mixture theory-based, reexamination and generalization of Biots model of acoustic propagation in saturated sand; Straughan's [23] in-depth book on waves in porous media; Jordan's [8] perturbation analysis of the Darcy-Jordan model (DJM) in the context of Stokes' second problem; the article by Ciarletta et al. [5] in which a study of anisotropic effects on poroacoustic acceleration waves is presented; and, more recently, the contribution by Fellah et al. [6] on the ultrasonic characterization of certain air-saturated porous materials.

* This work was supported by ONR/NRL funding (PE 061153N). All figures appearing herein were generated using the software package Mathematica.

Here, we consider acoustic traveling waves in a gas that saturates a rigid, stationary, porous medium. We carry out our analysis under the exact, fully nonlinear theory of homentropic[1] compressible flow; and we assume that Darcy's law [22], [14], [19],

$$\nabla P = -\Big(\frac{\mu\chi}{K}\Big)\mathbf{v}, \tag{1.1}$$

describes the drag exerted by the porous matrix on the gas flowing through it. In this note, P is an intrinsic pressure; ϱ is the mass density of the gas; we observe that the Darcy (or filtration) velocity vector $\boldsymbol{\mathcal{V}}$ is related to the intrinsic (i.e., volume-averaged over a volume element consisting of gas only) velocity vector $\mathbf{v}$ by the Dupuit-Forchheimer relationship, specifically, $\boldsymbol{\mathcal{V}} = \chi\mathbf{v}$; and the positive constants μ, K, and $\chi(< 1)$ denote the dynamic viscosity, permeability, and porosity, respectively.

It must be stressed that, since Darcy's law is just an approximation, based on many assumptions, some severe, to the balance of linear momentum, it does not have the same status as a balance law; see Rajagopal [17] for an excellent discussion of this point. Indeed, Beavers and Sparrow [1] point out that Darcy's law is applicable *only* in situations where the following inequality is satisfied:

$$(\mathrm{Re}_K)^{-1} \gg C_{\mathrm{f}}, \tag{1.2}$$

where the positive constant C_{f} denotes the form-drag (or inertia) coefficient that appears in the nonlinear drag law known as Forchheimer's equation (see (5.1)) and $\mathrm{Re}_K \propto \sqrt{K}$ (see (2.8)) is known as the permeability-based Reynolds number [3].

Our primary aim here is to extend and refine Jordan's [7] investigation of poroacoustic traveling waves under the DJM, a wave equation derived under weakly nonlinear theory, by forgoing all approximations to the governing equations. Specifically, exact TWSs for the case in which the saturating fluid is a perfect gas are derived and studied. In addition, special cases are considered, asymptotic/approximate results are presented, and numerical simulations are used to illustrate the main analytical findings. Most significantly, it is shown that, in addition to kinks, both shock and acceleration waves are possible, depending on the value of the speed of the traveling wave, and that, in the traveling wave context, the poroacoustic model considered here can be regarded as a generalization of that which describes acoustic propagation in certain mono-relaxing media.

To this end, the present note is arranged as follows. In Section 2, balance laws and constitutive assumptions are stated. In Section 3, an exact traveling wave analysis is carried out and graphs of the solution profiles are given. In Section 4, asymptotic

[1] For more on this special case of *isentropic* flow, see Thompson [24].

results are presented, special/limiting cases are noted, and discontinuities in the form of shock and acceleration waves are examined. Lastly, in Section 5, possible extensions of the present study are suggested and discussed.

2. Governing equations, basic assumptions, and nondimensionalizations

Consider a gas, which we take to behave as a perfect gas[2], that permeates a fixed and rigid, non-thermally conducting, homogeneous and isotropic porous medium. Assuming the gas is initially in its equilibrium state, and that the flow can be regarded as homentropic, the equations of continuity, momentum, and state are, in the case of one-dimensional (1D) flow along the x-axis, given by

$$\varrho_t + u\varrho_x + \varrho u_x = 0, \tag{2.1}$$

$$\varrho(u_t + uu_x) = -\wp_\varrho \varrho_x - \Big(\frac{\mu\chi}{K}\Big)u, \tag{2.2}$$

$$\wp = \wp_0(\varrho/\varrho_0)^\gamma, \tag{2.3}$$

where the assumption of homentropic flow means that $\eta = \eta_0$ throughout the entire volume of gas for all $t \geqslant 0$. Here, $\varrho(> 0)$ is the mass density; $\wp(> 0)$ is the thermodynamic pressure, where $\wp_\varrho$ denotes $\partial\wp/\partial\varrho$; the velocity vector has the form $\mathbf{v} = (u(x,t), 0, 0)$, which implies the velocity field is irrotational; η denotes the specific entropy; $\gamma = c_p/c_v$ is the adiabatic index, where the constants $c_p > c_v > 0$ respectively denote the specific heats at constant pressure and volume; and all body forces have been neglected. And by equilibrium state we mean the unperturbed state in which $u = 0$, $\varrho = \varrho_0$, $\wp = \wp_0$, and $\eta = \eta_0$ all hold simultaneously, where ϱ_0, $\wp_0$, and η_0 are constants.

To simplify the forthcoming analysis, we use the fact that $\wp_\varrho = c_0^2(\varrho/\varrho_0)^{\gamma-1}$, where the adiabatic sound speed $c_0 = \sqrt{\gamma\wp_0/\varrho_0}$ denotes the speed of sound in the undisturbed gas, and introduce the following non-dimensional quantities:

$$u^\circ = u/V, \quad \varrho^\circ = s + 1 = \varrho/\varrho_0, \quad \wp^\circ = \wp/\wp_0, \quad x^\circ = x/L, \quad t^\circ = c_0 t/L, \tag{2.4}$$

where the positive constants V and L denote a characteristic speed and length, respectively, and for future reference we note that s is the *condensation*, to recast (2.1)–(2.3) in the somewhat simpler (i.e., dimensionless) form

$$\varrho_t + \varepsilon(u\varrho)_x = 0, \tag{2.5}$$

$$\varrho(\varepsilon u_t + \varepsilon^2 uu_x) = -\varrho_x\varrho^{\gamma-1} - \varepsilon\delta u, \tag{2.6}$$

$$\wp = \varrho^\gamma. \tag{2.7}$$

[2] That is, an ideal gas for which the specific heats, and therefore their ratio, are constants; again, see Thompson [24, p. 79].

Here, $\varepsilon = V/c_0$ is the Mach number; $\delta = \chi/\operatorname{Re}$ is the dimensionless Darcy coefficient, where $\operatorname{Re} = c_0(K/L)/\nu$ is a Reynolds number and $\nu = \mu/\varrho_0$ denotes the kinematic viscosity; and all circle superscripts ($^\circ$) have been suppressed, but remain understood.

R e m a r k 1. The continuum assumption, on which our poroacoustic model is based, requires $\operatorname{Kn} \ll 1$, where $\operatorname{Kn} = \sqrt{K}/L$ is the Knudsen number of the flow considered here. Thus, δ can be re-expressed as

$$\delta = \varepsilon(\chi^2/\operatorname{Kn})/\operatorname{Re}_K\,. \tag{2.8}$$

3. Traveling wave analysis

3.1. Ansatzs

Let us assume $\varrho = f(\xi)$, $u = g(\xi)$, and $\wp = p(\xi)$, where $\xi := x - ct$ is the wave variable and, unless otherwise noted, the wave speed $c(:=$ const.$)$ is taken to be *positive*. On substituting the first two of these ansatzs into (2.5) and (2.6), integrating the former with respect to ξ, and then simplifying, the following system is obtained:

$$f(\varepsilon g - c) = \mathfrak{K}_1, \tag{3.1}$$

$$\varepsilon g' f(-c + \varepsilon g) + f^{\gamma-1} f' = -\varepsilon\delta g, \tag{3.2}$$

where $\mathfrak{K}_1$ is a constant of integration, a prime denotes $\mathrm{d}/\mathrm{d}\xi$, and we note for future reference that

$$p(\xi) = f^\gamma(\xi) \quad \text{and} \quad p'(\xi) = \gamma f^{\gamma-1}(\xi) f'(\xi). \tag{3.3}$$

Solving for $\mathfrak{K}_1$ using the equilibrium state conditions $f = 1$ and $g = 0$, (3.1) can be recast as

$$\varepsilon g = c(f-1)/f \quad (g < c/\varepsilon), \tag{3.4}$$

where the restriction now imposed on g ensures $f > 0$. On eliminating g between (3.2) and (3.4) using the fact that

$$\varepsilon g' = c f'/f^2, \tag{3.5}$$

we obtain, after simplifying, the *associated* ordinary differential equation (ODE) for the density, namely,

$$(1 - c^{-2} f^{\gamma+1}) f' = -\kappa f(1-f), \tag{3.6}$$

where we have set $\kappa := \delta/c$ for convenience.

R e m a r k 2. For simplicity of presentation in what follows, we introduce the quantity U, defined here as

$$U(\xi) := 1 - c^{-1}\varepsilon g = 1/f \quad (0 < f \leqslant U < \infty), \tag{3.7}$$

which will be used in *lieu* of g in graphs comparing the density and velocity fields. In terms of U, which can be regraded as the dimensionless specific volume [24, p. 53], (3.6) becomes

$$(1 - c^{-2}U^{-\gamma-1})U' = -\kappa(1 - U), \tag{3.8}$$

where we observe that $U = f = 1$ when the gas is in its equilibrium state.

3.2. Phase plane analysis and stability of equilibria

An analysis of (3.6) in the (f, f')-plane reveals that it admits the equilibrium solutions $\overline{f} = \{0, 1\}$, where it should be noted $\overline{f} = 0$ is always stable or unstable, respectively when $c > 0$ or $c < 0$. Moreover, if $f_{\rm w} \in (0, 1)$, where $f_{\rm w} := f(0)$ denotes that value of f at the wavefront $x = ct$, then $f \in (0, 1]$ for every $c > 0$. More importantly, however, (3.6) is found to describe *two* distinct flow regimes, corresponding to the two cases of $c \neq 1$, separated by the degenerate case $c = 1$.

For $c > 1$, the equilibrium solutions $\overline{f} = \{0, 1\}$ are stable and unstable, respectively, and, provided $f_{\rm w} \in (0, 1)$, there exists a unique, strictly decreasing kink-type solution of (3.6) such that $f \in (0, 1)$ for every $\xi \in \mathbb{R}$.

In contrast, when $c < 1$ it is easily established that $\overline{f} = \{0, 1\}$ are *both* stable and that at $f = f_{\rm s}$, where $f_{\rm s} := c^{2/(\gamma+1)}$ is a non-removable singular point of (3.6), $|f'| = \infty$. In fact, as we will soon see, f is *dual*-valued when $c < 1$ and $f_{\rm w} \in (0, 1)$ hold simultaneously.

For $c = 1$, f' exhibits a jump discontinuity at $\overline{f} = 1$, where it is noteworthy that the stability/instability of $\overline{f} = 1$ in this case *cannot* be determined. To understand the impact of this degeneracy, we need only re-express the $c = 1$ case of (3.6) as

$$(1 - f)\Big\{(\gamma + 1)\Big[1 - \frac{1}{2}\gamma(1 - f) + \frac{1}{6}\gamma(\gamma - 1)(1 - f)^2 + \ldots\Big]f' + \kappa f\Big\} = 0 \quad (c = 1), \tag{3.9}$$

from which it is evident that $f = 1$ is a solution, and then observe that

$$\lim_{f \to 1} \frac{f(1 - f)}{1 - f^{\gamma+1}} = \frac{1}{\gamma + 1}. \tag{3.10}$$

3.3. Exact solutions

Henceforth restricting our attention to bounded solutions, we return to (3.6) and integrate. Thus, we are led to consider the quadrature

$$\int_{f_{\mathrm{w}}}^{f} \frac{(1-c^{-2}\mathfrak{f}^{\gamma+1})\,\mathrm{d}\mathfrak{f}}{\mathfrak{f}(1-\mathfrak{f})} = -\kappa\xi, \quad \text{where } f_{\mathrm{w}} \in (0,1). \tag{3.11}$$

Observing that the integrand in (3.11) can *never* be a quotient of polynomials, since $1 < \gamma < 1.7$ in the case of perfect gases, this integral can, nevertheless, be evaluated exactly in terms of special functions.

Omitting the detail, it is readily established that the exact, albeit implicit, solution of (3.6) is given by the following.

For $c \neq 1$:

$$\frac{{}_2F_1(\gamma+1,1;\gamma+2;f)f^{\gamma+1} - {}_2F_1(\gamma+1,1;\gamma+2;f_{\mathrm{w}})f_{\mathrm{w}}^{\gamma+1}}{c^2(\gamma+1)} + \ln\Big[\frac{f_{\mathrm{w}}(1-f)}{f(1-f_{\mathrm{w}})}\Big] = \kappa\xi, \quad f \in (0,1). \tag{3.12}$$

For $c = 1$:

$$f(\xi) = 1, \quad \xi \in (-\infty, \xi_1(f_{\mathrm{w}})], \qquad \frac{{}_2F_1(\gamma+1,1;\gamma+2;f)f^{\gamma+1} - {}_2F_1(\gamma+1,1;\gamma+2;f_{\mathrm{w}})f_{\mathrm{w}}^{\gamma+1}}{\gamma+1} + \ln\Big[\frac{f_{\mathrm{w}}(1-f)}{f(1-f_{\mathrm{w}})}\Big] = \delta\xi, \quad f \in (0,1) \Rightarrow \xi \in (\xi_1(f_{\mathrm{w}}), \infty). \tag{3.13}$$

Here, ${}_2F_1$ denotes the Gauss hypergeometric series and

$$\xi_c(f_{\mathrm{w}}) = \frac{1}{c\delta}\Big[c^2 \ln\Big(\frac{f_{\mathrm{w}}}{1-f_{\mathrm{w}}}\Big) - \lambda - \psi(\gamma+1) - \frac{{}_2F_1(\gamma+1,1;\gamma+2;f_{\mathrm{w}})f_{\mathrm{w}}^{\gamma+1}}{\gamma+1}\Big], \tag{3.14}$$

where $\psi(\cdot)$ is the digamma function and $\lambda \approx 0.5772$ is the Euler-Mascheroni constant.

Regarding the velocity and pressure fields, we observe that the corresponding exact, but implicit, expressions for g and p can be derived using (3.4) and (3.3), respectively, where it should be noted that $0 < p \leqslant f \leqslant 1$.

In the case of the quantity U, it is not difficult to show that (3.8), like (3.6), can be integrated in terms of special functions; e.g., for $c \neq 1$:

$$-\Big[\frac{{}_2F_1(1-\gamma,1;2-\gamma;\mathfrak{U})\mathfrak{U}^{1-\gamma}}{c^2(\gamma-1)} - \ln(\mathfrak{U}-1) + \gamma^{-1}c^{-2}\mathfrak{U}^{-\gamma}\Big]\Big|_{1/f_{\mathrm{w}}}^{U} = \kappa\xi, \quad U \in (1,\infty), \tag{3.15}$$

which like its counterpart (3.12) is an exact, but implicit, result. Here, $U(0) = 1/f_{\mathrm{w}}$ is the required wavefront condition.

3.4. Numerical results: Integral curves

In this subsection we plot the f vs. ξ and U vs. ξ solution profiles for both diatomic and monatomic gases. The four figures presented here cover the cases $c \neq 1$ and $c = 1$ and, apart from the values chosen for γ, the curves they contain do not necessarily depict a particular poroacoustic flow situation. Lastly, it should be noted that, since the associated ODEs are invariant under $\xi \mapsto \xi + \text{const.}$, we take, without loss of generality, $f_{\mathrm{w}} = 1/2$ in Figs. 1–4, and also in Fig. 5, which appears in Subsection 4.4.3 below.

In Fig. 1 we have plotted, for a gas with $\gamma = 7/5$ (e.g., air at 20 °C), the expressions given in (3.12) and (3.15) for $c > 1$. Clearly, the density profile assumes the form of a kink, as we inferred from our stability analysis, whose amplitude tends to zero (i.e., the vacuum state) as $\xi \to \infty$. The U vs. ξ profile, on the other hand, is seen to blow-up as $\xi \to \infty$, i.e., as the density tends to the vacuum state, which is consistent with the behavior of the velocity field reported in [7]; see Remark 3 below.

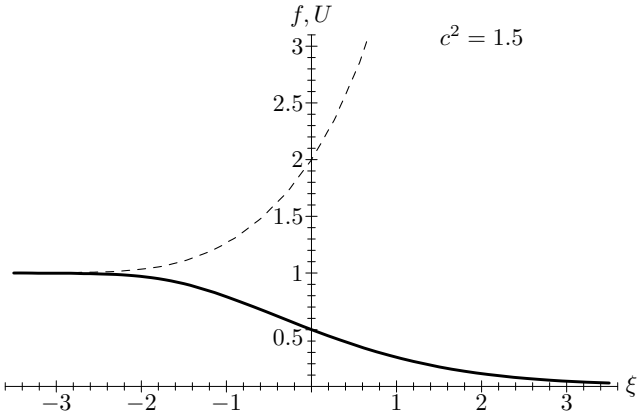

Figure 1. f, U vs. ξ for $c \approx 1.225$, $\gamma = 7/5$, $f_{\mathrm{w}} = 0.5$, and $\kappa = 1$. Solid curve: (3.12). Broken curve: (3.15).

In contrast, Fig. 2 clearly illustrates the fact, alluded to in Subsection 3.2, that f is dual-valued when $c < 1$ and $f_{\mathrm{w}} \in (0, 1)$ hold simultaneously. Here, assuming once again $\gamma = 7/5$, we have plotted f vs. ξ for three different values of $c < 1$, but fixed f_{w}. While such non-unique solutions are acceptable from the mathematical standpoint, they are, of course, physically unrealistic. As we will see in Subsection 4.3.2, however, for $c < 1$ (3.12) actually represents a discontinuous waveform, known as an *inner discontinuity* [26, p. 77], the physical interpretation of which is a shock wave.

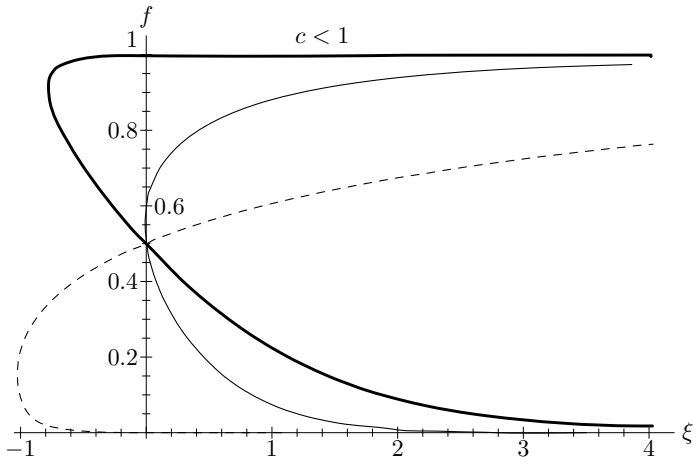

Figure 2. f vs. ξ generated from (3.12) for $\gamma = 7/5$, $f_{\mathrm{w}} = 0.5$, and $\kappa = 1$. Bold-solid curve: $c = 0.9$. Thin-solid curve: $c = 0.5$. Broken curve: $c = 0.1$.

The sequence shown in Fig. 3, in which the gas phase is taken to be CO_2 at several thousand degrees Kelvin [24, p. 80], illustrates the transition from the smooth kink

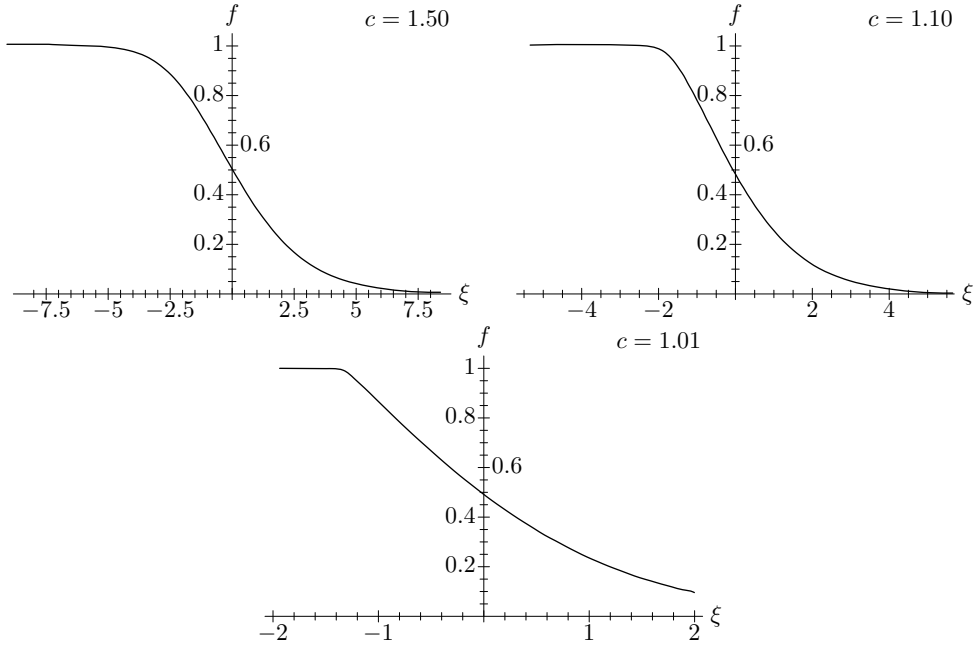

Figure 3. f vs. ξ for $\gamma = 15/13$, $f_{\mathrm{w}} = 0.5$, and $\kappa = 1.0$.

generated by (3.12) to the piecewise-defined profile described by (3.13) as $c \to 1$ (from above). In particular, we observe that the f vs. ξ profile forms a corner in this

limit, thus implying that f' develops a jump discontinuity as $c \to 1$, the location of which (in this figure) *will* be $\xi = \xi_1(0.5) \approx -1.258$.

In Fig. 4 we have plotted the f vs. ξ and U vs. ξ profiles for the actual case $c = 1$, but where a monatomic gas (e.g., Ar, He, etc.) is now assumed, using the piecewise-defined, but continuous, expression given in (3.13). Here, we see that the aforementioned corner is now fully formed, and located at $\xi = \xi_1(0.5)$ in the present figure. Moreover, the U profile is also seen to exhibit a corner, at the same location as f, and thus it follows that U' is also discontinuous. In Subsection 4.3.3 we will reexamine the $c = 1$ case using the singular surface theory and derive exact expressions for the jumps in f', g', and p'.

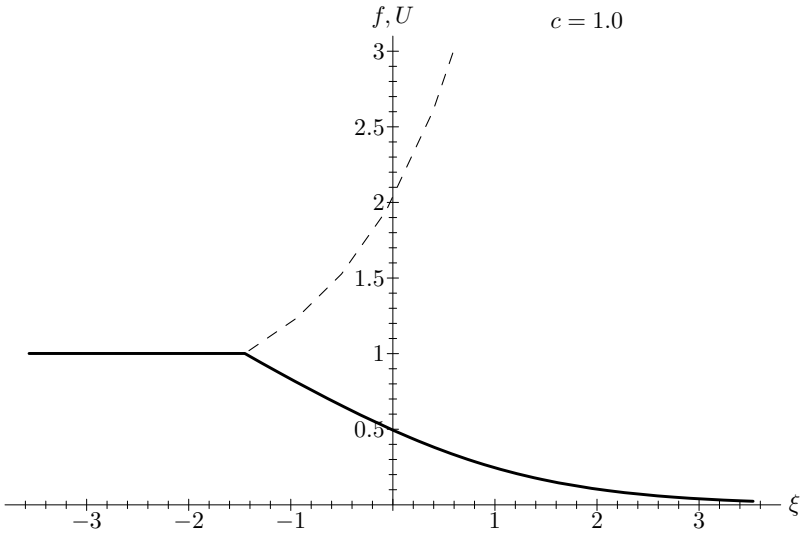

Figure 4. f, U vs. ξ for $c = 1.0$, $\gamma = 5/3$, $f_{\mathrm{w}} = 0.5$, and $\delta = 1$. Solid curve: (3.13). Broken curve: $U(\xi) = 1/f(\xi)$, where f is given by (3.13).

4. Analytical results

4.1. Asymptotics of the kink profiles

To gain a better understanding of the behavior of our model, we present in this subsection large-$|\xi|$ and small-$|\xi|$ expressions for the cases $c \geqslant 1$. These expressions, which are not only explicit, but much simpler than their exact counterparts, were derived based on truncated expansions of either the corresponding case of the exact solution given in Subsection 3.3, or of the integrand in (3.11). And while the following relate only to f, parallel expressions for g and p can, of course, be derived using (3.4) and (3.3), respectively.

For $c > 1$:

$$(4.1)\quad f(\xi) \sim \begin{cases} 1 - \exp\Big[\dfrac{c\delta[\xi - \xi_c(\frac{1}{2})]}{c^2 - 1}\Big], & \xi \to -\infty, \\ \dfrac{2^\gamma c^2[2 + \gamma 2^{-\gamma} c^{-2} - \sqrt{(2 - 2^{-\gamma}c^{-2})^2 + 2^{1-\gamma}c^{-3}\delta\xi}]}{2(\gamma+1)}, & |\xi| \to 0, \\ \exp\Big\{-\Big[\dfrac{{}_2F_1(\gamma+1, 1; \gamma+2; \frac{1}{2})(\frac{1}{2})^{\gamma+1} + c\delta(\gamma+1)\xi}{c^2(\gamma+1)}\Big]\Big\}, & \xi \to \infty. \end{cases}$$

For $c = 1$:

$$(4.2)\quad f(\xi) \simeq \begin{cases} 1, & \xi \leqslant \xi_1(\frac{1}{2}), \\ 1 + \dfrac{2\{(\gamma+1) - \sqrt{(\gamma+1)^2 + \delta P(\gamma)[\xi - \xi_1(f_{\rm w})]}\}}{P(\gamma)}, & \xi_1(\frac{1}{2}) < \xi \ll 0, \\ \dfrac{2^\gamma[2 + \gamma 2^{-\gamma} - \sqrt{(2 - 2^{-\gamma})^2 + 2^{1-\gamma}\delta\xi}]}{2(\gamma+1)}, & |\xi| \to 0^+, \\ \exp\Big\{-\Big[\dfrac{{}_2F_1(\gamma+1, 1; \gamma+2; \frac{1}{2})(\frac{1}{2})^{\gamma+1} + \delta(\gamma+1)\xi}{\gamma+1}\Big]\Big\}, & \xi \to \infty. \end{cases}$$

Here, we have set $P(\gamma) := (\gamma+1)(2-\gamma)$ and, for simplicity of presentation, we have again taken $f(0) = 1/2$.

R e m a r k 3. From $(4.1)_3$, $(4.2)_3$, and the relation $U = 1/f$, the blow-up of U depicted in Figs. 1 and 4 is easily seen to be exponential, specifically, like

$$(4.3)\qquad U(\xi) \sim \exp\Big[\frac{{}_2F_1(\gamma+1, 1; \gamma+2; \frac{1}{2})(\frac{1}{2})^{\gamma+1} + c\delta(\gamma+1)\xi}{c^2(\gamma+1)}\Big] \quad (\xi \to \infty),$$

where the former and latter respectively correspond to $c = \sqrt{1.5}$ and $c = 1$.

R e m a r k 4. When c is large, (3.12) admits the following simple approximation:

$$(4.4)\qquad f(\xi) \approx \frac{1}{2}\Big[1 - \tanh\Big(\frac{1}{2}\kappa\xi\Big)\Big] \quad (c \gg 1),$$

which of course represents a Taylor shock of shock thickness $4/\kappa$. Since it does not appear, either explicitly or implicitly, in (4.4), we see that f, g, and p are all highly *insensitive* to changes in γ when $c \gg 1$. Thus, according to our model, all perfect gases exhibit, qualitatively speaking, the same behavior in the large-c regime.

4.2. Special cases of perfect gases

In the case of monatomic (e.g., noble gases) and diatomic (e.g., nitrogen, oxygen, CO_2) gases under ordinary conditions, $\gamma = 5/3$ and $\gamma = 7/5$, respectively; see [24,

p. 80]. For these two important subclasses of perfect gases, the integral in (3.11) can be evaluated in terms of elementary functions.

For $\gamma = 5/3$:

$$\Big[\ln\Big(\frac{1-\mathfrak{f}}{\mathfrak{f}}\Big) - \frac{3}{10}c^{-2}\mathfrak{f}^{2/3}(5+2\mathfrak{f}) - c^{-2}\sqrt{3}\arctan\Big(\frac{1+2\mathfrak{f}^{1/3}}{\sqrt{3}}\Big) - c^{-2}\ln\Big(\frac{1-\mathfrak{f}^{1/3}}{\sqrt{1+\mathfrak{f}^{1/3}+\mathfrak{f}^{2/3}}}\Big)\Big]\Big|_{f_{\rm w}}^{f} = \kappa\xi. \tag{4.5}$$

For $\gamma = 7/5$:

$$\Big\{\ln\Big(\frac{1-\mathfrak{f}}{\mathfrak{f}}\Big) - c^{-2}\Big[\ln(1-\mathfrak{f}^{1/5}) + \frac{5}{14}\mathfrak{f}^{2/5}(7+2\mathfrak{f}) - \sqrt{\varphi^{-1}\sqrt{5}}\arctan\Big(\frac{2\mathfrak{f}^{1/5}-\varphi^{-1}}{\sqrt{\varphi\sqrt{5}}}\Big) + \sqrt{\varphi\sqrt{5}}\arctan\Big(\frac{2\mathfrak{f}^{1/5}+\varphi}{\sqrt{\varphi^{-1}\sqrt{5}}}\Big) - \frac{1}{2}\varphi\ln(1-\varphi^{-1}\mathfrak{f}^{1/5}+\mathfrak{f}^{2/5}) + \frac{1}{2}\varphi^{-1}\ln(1+\varphi\mathfrak{f}^{1/5}+\mathfrak{f}^{2/5})\Big]\Big\}\Big|_{f_{\rm w}}^{f} = \kappa\xi, \tag{4.6}$$

where $\varphi = (1+\sqrt{5})/2$ is the Golden ratio. Here, it must be stressed that these expressions are valid only for the cases $c \neq 1$; however, their specialization to $c = 1$ is easily accomplished with the aid of (3.13).

4.3. Shock and acceleration waves

We now investigate the range of shock and acceleration wave phenomena admitted by our Darcy-based model under the traveling wave assumption. First, however, it is necessary to introduce three important concepts from the theory of singular surfaces [25], [23].

(i) The plane $x = \Sigma(t)$ represents a singular surface, which in the present study propagates to the right along the x-axis with speed c, across which some function, say, $\mathfrak{F} = \mathfrak{F}(x,t)$, suffers a jump discontinuity.

(ii) The *amplitude* of this jump in $\mathfrak{F}$ is defined as $[\![\mathfrak{F}]\!] := \mathfrak{F}^- - \mathfrak{F}^+$, where $\mathfrak{F}^\pm := \lim_{x\to\Sigma^\pm}\mathfrak{F}$ are assumed to exist and $\pm$ superscripts correspond to the regions ahead of and behind Σ, respectively.

(iii) And by a *shock wave* we mean here a propagating singular surface (i.e., a wavefront) across which f (and thus g, p) suffer a jump discontinuity.

4.3.1. Shock waves: $c \geqslant 1$. Although they are, perhaps, less interesting than those which arise when $c < 1$, shocks can also form in the kink profiles, i.e., for $c \geqslant 1$,

but only in the limit $\delta \to \infty$. This follows from the fact that the *shock thickness*, l (> 0) [16], which for $f(0) = 1/2$ is given by

$$l = 4c\delta^{-1}\Big[1 - c^{-2}\Big(\frac{1}{2}\Big)^{\gamma+1}\Big] \quad (c \geqslant 1), \tag{4.7}$$

tends to zero as $\delta \to \infty$. In term of the viscosity, a shock forms as μ becomes very large, provided $c \geqslant 1$, under our poroacoustic model. Clearly, this behavior is the exact *opposite* of what occurs in classical (i.e., nonporous) gas dynamics, where a shock forms as $\mu \to 0$. As Rajagopal [17] has pointed out, however, one of the key assumptions underpinning Darcy's law is that viscous dissipation within the mass of fluid itself is negligibly small. Thus, from the physical standpoint, letting $\mu \to \infty$ in this (or any) Darcy-based model will almost certainly yield unrealistic results.

4.3.2. Shock waves: $c < 1$. As noted earlier, the physical interpretation of the dual-valued waveforms shown in Fig. 2 is that they represent shock waves. Weakly nonlinear shock theory can be used, as it is in the case of acoustic traveling waves in mono-relaxing media, to "correct" the $c < 1$ case of (3.12), whereby a single-valued, but discontinuous, expression is obtained.

While an in-depth study of this case cannot be carried out here due to limited space, we can give, with the help of [16], the shock amplitude expressions predicted by the weakly nonlinear version of our model. Thus, on expanding about $\overline{f} = 1$ and neglecting the appropriate higher-order terms, it follows that solutions of (3.6) can be approximated by those of the Abel equation:

$$(\sigma - f)f' = -\frac{1}{2}c\delta\beta^{-1}f(1-f), \quad \text{where } \sigma := 1 - \frac{1}{2}\beta^{-1}(1-c^2). \tag{4.8}$$

The coefficient of nonlinearity, β (> 1) [2], has been introduced here because (4.8), being derived under a weakly nonlinear approximation[3], is applicable to *both* gases and liquids, where $\beta = (\gamma + 1)/2$ in the case of the former; in fact, this ODE can also be used to determine the acceleration wave amplitudes given below in Subsection 4.3.3. Thus, the findings reported in the remainder of this section (4) apply to both gases *and* liquids, via the fact that they are expressed in terms of β.

Since (4.8) is identical in form to [16, Eq. (11-6.19)], it is a relatively straightforward matter now to construct the corrected waveform for $c < 1$ and show that the

[3] Also known as a "finite-amplitude" approximation, it is based, in the case of homentropic flow, on the use of the quadratic power series expansion $\wp \approx \wp_0 + \varrho_0 c_0^2[s + (\beta - 1)s^2]$, expressed here in *dimensional* form, and where s is defined in Eq. (2.4), in place of (2.3); see [11], [2], [4].

resulting shock amplitudes are given by

$$\llbracket f \rrbracket = \frac{1-c^2}{\beta}, \qquad \llbracket U \rrbracket = \frac{-(1-c^2)}{\beta-(1-c^2)}, \tag{4.9}$$
$$\llbracket p \rrbracket = \frac{(2\beta-1)(1-c^2)}{\beta}\Big[1-\frac{(\beta-1)(1-c^2)}{\beta}\Big] \qquad (c<1).$$

Here, $f^- = 1$, since Σ is propagating to the right; $f^+ = 1-(1-c^2)/\beta$, where the condition $\lim_{\xi\to 0^+} f(\xi) = f^+$ was imposed to place the shock-front at $\xi = 0$; $\llbracket U \rrbracket$ was determined using the relation $U = 1/f$ in conjunction with the jump product rule

$$\llbracket \mathfrak{A}\mathfrak{B} \rrbracket = \mathfrak{A}^+ \llbracket \mathfrak{B} \rrbracket + \mathfrak{B}^+ \llbracket \mathfrak{A} \rrbracket + \llbracket \mathfrak{A} \rrbracket \llbracket \mathfrak{B} \rrbracket; \tag{4.10}$$

$\llbracket p \rrbracket$ was obtained by expanding $(3.3)_1$ about $\overline{f} = 1$; and we observe that $\llbracket f \rrbracket \in (0,1)$, $\llbracket U \rrbracket \in (-(\beta-1)^{-1}, 0)$, and $\llbracket p \rrbracket \in (0,1)$.

4.3.3. Acceleration waves. Along with shock waves, compressible flows can also support acceleration waves [25], [23]. In the present study, such waves arise *only* when $c = 1$ and correspond to jumps in f', g', etc., across the plane $\xi = \xi_1(f_{\rm w})$. Making the identification $\Sigma(t) = t + \xi_1(f_{\rm w})$ and noting that $(f')^- = 0$, it can be shown that

$$\llbracket f' \rrbracket = \frac{\delta}{2\beta}, \quad \llbracket g' \rrbracket = \frac{\delta}{2\varepsilon\beta}, \quad \llbracket p' \rrbracket = \frac{\delta(2\beta-1)}{2\beta} \qquad (c=1), \tag{4.11}$$

where $\llbracket g' \rrbracket$ and $\llbracket p' \rrbracket$ were determined using (3.5) and $(3.3)_2$, respectively, along with the aid of $(4.11)_1$ and (4.10).

In Fig. 5 we give an example of an acceleration wave in the density, where we note that $-f'$ here corresponds to ϱ_t since $c = 1$, for the case in which the gas phase is assumed to be a diatomic gas (e.g., N_2 [24, p. 80]) under ordinary conditions. For these parameter values, the wavefront in Fig. 5 is located at $\xi = \xi_1(0.5) \approx -1.355$, which follows from (3.14), and the acceleration wave amplitude is $\llbracket f' \rrbracket \approx 0.417$, in agreement with $(4.11)_1$.

Turning now to Hadamard's lemma [25], it is not difficult to show that $\llbracket \varrho_t \rrbracket = -\llbracket f' \rrbracket$ and $\llbracket u_t \rrbracket = -\llbracket g' \rrbracket$ when $c = 1$. Thus, we find that

$$\llbracket u_t \rrbracket = -\alpha^* \quad (c=1), \tag{4.12}$$

where $\alpha^* = \delta/(2\varepsilon\beta)$ is a critical amplitude value (see, e.g., [7]).

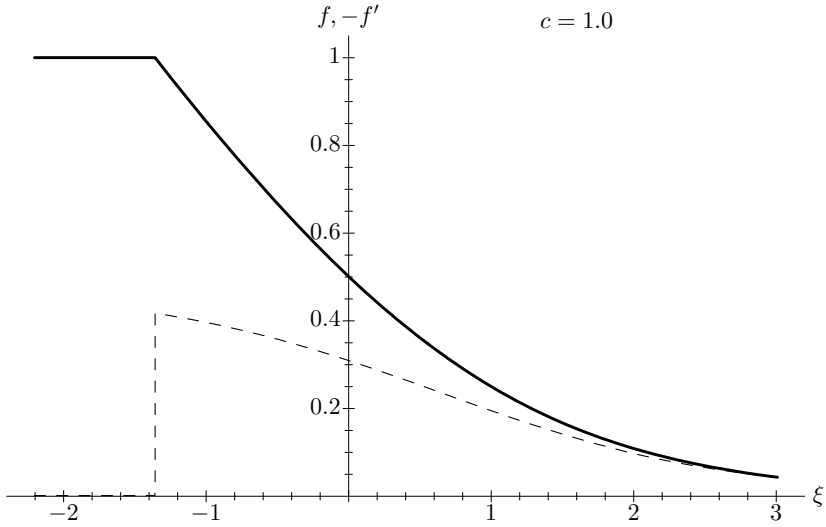

Figure 5. f, $-f'$ vs. ξ for $c = 1.0$, $\gamma = 7/5$ (i.e., $\beta = 1.2$), $f_{\mathrm{w}} = 0.5$, and $\delta = 1.0$. Solid curve: f vs. ξ. Broken curve: $-f'$ vs. ξ.

R e m a r k 5. From (4.12) it is clear that the DJM of [7] and the exact model of the present note predict the same value for the acceleration wave's magnitude, but *not* its amplitude. This discrepancy in sign is easily resolved by observing that $\mathcal{U}$, the quantity in the former corresponding to g here, is non-negative, a result of the fact that $\mathcal{U}(0) > 0$ was *assumed* in [7].

4.4. Weakly nonlinear theory and connections to other fields

The weakly nonlinear versions of the associated ODEs for f and g are the Abel equations

$$(4.13) \qquad (\sigma - f)f' = -\frac{1}{2}c\delta\beta^{-1}f(1-f) \quad \text{and} \quad [(1-c^2) + 2c^{-1}\varepsilon\beta g]g' = -c\delta g.$$

Clearly, the former is just (4.8), re-stated here for the reader's convenience, while the latter, which except for the coefficient of g on the left-hand side is identical to its counterpart under the DJM [7, Eq. (9)], is based on the assumption $\varepsilon|g| \ll c$.

It is noteworthy that, along with problems involving traffic flow and atmospheric (traveling) waves, $(4.13)_1$ also arises, as the reader might have already inferred, when considering acoustic traveling waves in mono-relaxing media; see [9] and references therein. Thus, in the traveling wave context, we see that the weakly nonlinear version of our poroacoustic model is, from the mathematical standpoint, equivalent to those of the three examples just cited.

We close this section with the observation that *explicit* solutions of $(4.13)_1$ and $(4.13)_2$ can be expressed approximately [9] and exactly [7], respectively, in terms of the Lambert W-function, the "W-function" being a recent addition to the family of special functions which is rapidly being put to use by researchers from many different fields (see [21], [7], [4], [9] and references therein).

5. Extensions, modifications, and possible future work[4]

While Darcy's law is the oldest and best known model of flow in porous media, it does, as noted in Section 1, have its limitations. Consequently, since the early part of the 20th century an array of modifications and alternatives to (1.1) have been proposed, the best known of these being the equations of Forchheimer and Brinkman.

In situations involving high-velocity flow through porous materials, i.e., the velocity regime in which the inequality in (1.2) is *not* satisfied, Darcy's law has been shown to fail [22], [14]. In such cases, the current consensus in literature is that Forchheimer's equation, the most common version of which is [14]

$$\nabla P = -\Big(\frac{\mu\chi}{K}\Big)\mathbf{v} - \varrho(C_{\mathrm{f}}\chi^2 K^{-1/2})|\mathbf{v}|\mathbf{v}, \tag{5.1}$$

then becomes the appropriate form of the resistance law. With regards to the present investigation, it is noteworthy that a precedent supporting the application of (5.1) to *subsonic* compressible flows can be found in literature; again, see [1].

However, if a boundary or an interface is present, or if the porosity is very close to unity, then, as pointed out by Payne et al. [15], there is a school of thought that contends that Brinkman's equation (see, e.g., [14] and references therein)

$$\nabla P = \tilde{\mu}\chi\boldsymbol{\nabla}^2\mathbf{v} - (\mu\chi K^{-1})\mathbf{v}, \tag{5.2}$$

where $\tilde{\mu}$ (> 0) is an effective viscosity known as the *Brinkman* viscosity, should be used in place of (1.1). With regards to using Brinkman's equation to describe poroacoustic phenomena, we refer the reader to [8, Section 5.2], wherein a weakly nonlinear model, based on the 1D case of (5.2), is presented.

And finally, along with including thermal effects, which can be significant in many geophysical applications [18], and combining (5.1) and (5.2) into a single resistance law, one could also re-work the present traveling wave analysis for the case of poroacoustic propagation in a gas with pressure dependent viscosity. For as pointed out

[4] In this, the final section, we revert back to using *dimensional* quantities.

by Málek and Rajagopal [12, p. 383], in the case of a compressible viscous fluid, μ actually depends on the pressure. As an important step towards carrying out such a study, we point to the recent article by Kannan and Rajagopal [10]; in it a generalization of (5.2) is derived, which we term the Brinkman-Kannan-Rajagopal (BKR) equation, which allows for a pressure-dependent viscosity coefficient.

Acknowledgment. The authors thank Profs. P. Krejčí and J. Málek for their kind invitation to contribute to this special issue honoring Prof. Rajagopal. The authors also thank the two anonymous referees for their extremely helpful comments and suggestions.

References

[1] *G. S. Beavers, E. M. Sparrow*: Compressible gas flow through a porous material. Int. J. Heat Mass Transfer *14* (1971), 1855–1859.
[2] *R. T. Beyer*: The parameter B/A. In: Nonlinear Acoustics (M. F. Hamilton, D. T. Blackstock, eds.). Academic Press, San Diego, 1997, pp. 25–39.
[3] *K. Boomsma, D. Poulikakos*: The effects of compression and pore size variations on the liquid flow characteristics in metal foams. ASME J. Fluids Eng. *124* (2002), 263–272.
[4] *I. Christov, C. I. Christov, P. M. Jordan*: Modeling weakly nonlinear acoustic wave propagation. Q. J. Mech. Appl. Math. *60* (2007), 473–495.
[5] *M. Ciarletta, B. Straughan, V. Tibullo*: Anisotropic effects on poroacoustic acceleration waves. Mech. Res. Commun. *37* (2010), 137–140.
[6] *Z. E. A. Fellah et al.*: Ultrasonic characterization of air-saturated double-layered porous media in time domain. J. Appl. Phys. *108* (2010).
[7] *P. M. Jordan*: Finite-amplitude acoustic traveling waves in a fluid that saturates a porous medium: Acceleration wave formation. Phys. Lett. A *355* (2006), 216–221.
[8] *P. M. Jordan*: Some remarks on nonlinear poroacoustic phenomena. Math. Comput. Simul. *80* (2009), 202–211.
[9] *P. M. Jordan et al.*: On the propagation of finite-amplitude acoustic waves in mono-relaxing media. In: Continuum Mechanics, Fluids, Heat. Proceedings of the 5th IASME/WSEAS International Conference on Continuum Mechanics, Cambridge, UK, February 23–25, 2010 (S. H. Sohrab, H. J. Catrakis, N. Kobasko, eds.). WSEAS Press, Athens, 2010, pp. 67–72.
[10] *K. Kannan, K. R. Rajagopal*: Flow through porous media due to high pressure gradients. Appl. Math. Comput. *199* (2008), 748–759.
[11] *S. Makarov, M. Ochmann*: Nonlinear and thermoviscous phenomena in acoustics, Part I. Acta Acustica united with Acustica *82* (1996), 579–606.
[12] *J. Málek, K. R. Rajagopal*: Mathematical issues concerning the Navier-Stokes equations and some of its generalizations. In: Handbook of Differential Equations: Evolutionary Equations, Vol. 2 (C. M. Dafermos, E. Feireisl, eds.). Elsevier/North Holland, Amsterdam, 2005, pp. 371–459.
[13] *P. M. Morse, K. U. Ingard*: Theoretical Acoustics. McGraw-Hill, New York, 1968.
[14] *D. A. Nield, A. Bejan*: Convection in Porous Media, 2nd ed. Springer, New York, 1999.
[15] *L. E. Payne, J. F. Rodrigues, B. Straughan*: Effect of anisotropic permeability on Darcy's law. Math. Methods Appl. Sci. *24* (2001), 427–438.
[16] *A. D. Pierce*: Acoustics: An Introduction to its Physical Principles and Applications. Acoustical Society of America, Woodbury, 1989, pp. 588–593.

[17] *K. R. Rajagopal*: On a hierarchy of approximate models for flows of incompressible fluids through porous solids. Math. Models Methods Appl. Sci. *17* (2007), 215–252.
[18] *K. R. Rajagopal, G. Saccomandi, L. Vergori*: A systematic approximation for the equations governing convection-diffusion in a porous medium. Nonlinear Anal., Real World Appl. *11* (2010), 2366–2375.
[19] *K. R. Rajagopal, L. Tao*: Mechanics of Mixtures. Appendix B. World Scientific, Singapore, 1995.
[20] *K. R. Rajagopal, L. Tao*: On the propagation of waves through porous solids. Int. J. Non-Linear Mech. *40* (2005), 373–380.
[21] *U. Saravanan, K. R. Rajagopal*: On the role of inhomogeneities in the deformation of elastic bodies. Math. Mech. Solids *8* (2003), 349–376.
[22] *A. E. Scheidegger*: The Physics of Flow Through Porous Media, 3rd ed. University of Toronto Press, Toronto, 1974.
[23] *B. Straughan*: Stability and Wave Motion in Porous Media. Springer, New York, 2008.
[24] *P. A. Thompson*: Compressible-Fluid Dynamics. McGraw-Hill, New York, 1972.
[25] *C. Truesdell, K. R. Rajagopal*: An Introduction to the Mechanics of Fluids. Birkhäuser, Boston, 2000.
[26] *G. B. Whitham*: Linear and Nonlinear Waves. John Wiley & Sons, New York, 1974.

Authors' address: *P. M. Jordan*, *J. Fulford*, Acoustics Division, U. S. Naval Research Laboratory, Stennis Space Center, Mississippi 39529-5004, U.S.A, e-mail: `pjordan@nrlssc.navy.mil`; `jim.fulford@nrlssc.navy.mil`.